Polyhedron 249 (2024) 116793

Contents lists available at ScienceDirect

Polyhedron

journal homepage: www.elsevier.com/locate/poly

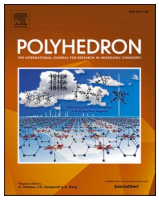

New hyaluronan-terpyridine conjugate: Metal complexes and their biological activity

Roberta Panebianco [a], Maurizio Viale [b], Graziella Vecchio [a,*]

[a] Dipartimento di Scienze Chimiche, Università degli Studi di Catania, Viale A. Doria 6, 95125 Catania, Italy
[b] IRCCS Ospedale Policlinico San Martino, U.O.C. Bioterapie, L.go R. Benzi 10, 16132 Genova, Italy

ARTICLE INFO

Keywords:
Cancer
Copper
Hyaluronic acid
Iron
Zinc

ABSTRACT

Terpyridine coordination compounds have attracted broad interest concerning their biomedical applications. We devised a terpyridine-hyaluronic acid conjugate and studied its copper(II), iron(II) and zinc(II) metal complexes. We determined the antiproliferative activities of the ligand and the metal complexes in human cell lines A2780 (ovary, adenocarcinoma), A549 (lung, carcinoma), MDA-MB-453 (breast, carcinoma), SKHep1 (liver, carcinoma) and compared them to 4′-Chloro-2,2′:6′,2″-terpyridine systems. The terpyridine-hyaluronan conjugate showed pharmacologically significant antiproliferative activity in all cell lines tested. The ternary metal complexes of terpyridine-hyaluronan conjugate and 4-chloro-terpyridine showed significant IC_{50} values (nanomolar range) depending on the cell line. Additionally, Cu^{2+} and Zn^{2+} ternary complexes exhibited higher antiproliferative activity than Doxorubicin.

1. Introduction

Metal complexes have been investigated as potential therapeutics because of their biological activity [1]. Despite the development of metallodrugs based on second or third-row transition metal ions, remarkable results have been obtained with new metallodrugs based on the naturally more abundant and intrinsically less toxic first-row transition metal ions. Zinc(II), copper(II), cobalt(II), and iron(II) are of primary consideration due to their biocompatibility and involvement in biological processes in the human body [2–5]. It has been observed that various coordination compounds containing these metals exhibit outstanding anticancer efficacy [6–10].

In this context, terpyridine (tpy) derivative coordination compounds have attracted wide interest concerning biomedical applications [4,9,11].

Terpyridine is an *N*-heterocycle pincer-ligand with a high binding affinity towards transition metal ions, such as iron(II), zinc(II), and copper(II). This characteristic has been widely used to build supramolecular systems, mainly soluble in organic solvents [12–14].

Tpy metal complexes have been used in medicinal chemistry because of their peculiar structure and range of biological activities [15–18]. Indeed, the anticancer activity of tpy and its coordination compounds has also been reported in recent years [19–22]. It has been proven that some tpy metal complexes could affect cell activity by inhibiting the normal function of nucleic acids and enzymes [18,23–27].

However, tpy metal complexes are hardly water-soluble, but their functionalisation can improve water solubility. It is known that the dissolution in aqueous media allows it to reach therapeutic concentration. Various approaches have been investigated to overcome the poor solubility issue and increase bioavailability [28,29].

Amongst them, carbohydrate conjugation stands out in obtaining new hybrids with improved solubility, bioavailability, enhanced biological activity and selective targeting properties [30,31].

Hyaluronic acid or hyaluronan (HA) is an endogenous polymer of D-glucuronic acid and *N*-acetyl-D-glucosamine [32,33]. HA is the principal component of the extracellular matrix (ECM) and is involved in different biological processes, such as cell proliferation and cell migration, and it regulates the inflammatory state of the ECM. Exogenous HA fragments of low molecular weight have been shown to affect cell behaviour through binding to CD44 and RHAMM (Receptor for Hyaluronan Mediated Motility) receptors [34].

In particular, the CD44 receptor belongs to a family of cell adhesion molecules [32,35]. It is a widely distributed transmembrane glycoprotein that plays a critical role in malignant cell activities, including adhesion, migration, invasion, and survival; it is also strongly implicated in the cell signalling cascades associated with cancer [36]. CD44 is a

* Corresponding author.
E-mail address: gr.vecchio@unict.it (G. Vecchio).

https://doi.org/10.1016/j.poly.2023.116793
Received 17 September 2023; Accepted 12 December 2023
Available online 14 December 2023
0277-5387/© 2023 The Author(s). Published by Elsevier Ltd. This is an open access article under the CC BY-NC-ND license (http://creativecommons.org/licenses/by-nc-nd/4.0/).

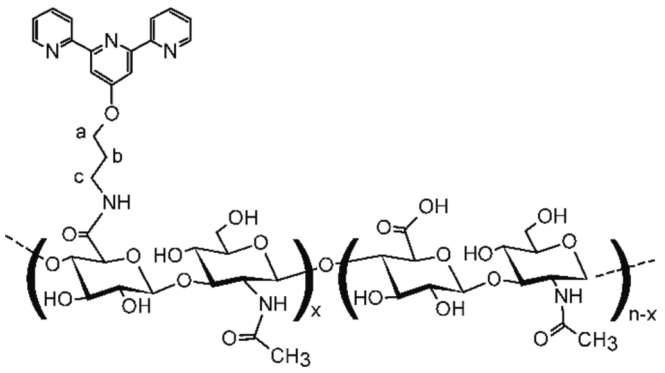

Fig. 1. Tpy conjugated with HA (n = 30, x = 7).

critical component in the internalisation and metabolism of HA and is expressed at low levels in various cell types. Tumour-derived cells, however, express CD44 in a high-affinity state that can promote the binding and internalisation of HA [33]. Aside from this targeting ability, HA nanosystems show several interesting features, such as very low immunogenicity, biodegradability, non-inflammatory reactions, bioavailability and biocompatibility [32,34]. Also, hyaluronidase degrades HA to low molecular weight components [34].

Due to these biological features, there is a prominent interest in obtaining HA-based functional biomaterials [34].

HA-based NPs have been widely used as drug delivery systems [37–40]. Specifically, HA-drug conjugates enhance drug circulation time, stability, solubility and accumulation in CD44 overexpressing cancer cells [40,41].

The HA affinity towards some biometals has also been studied [42–44]. Although, few derivatives of HA with metal chelators have been synthesised [45–47].

Based on the interest in HA properties, here we report a new multimetal system based on the coordination properties of tpy functionalising HA polymers (Fig. 1). Particularly, we functionalised low molecular weight HA (about 11 kDa) with tpy moieties to exploit the coordination ability of tpy in aqueous solutions. We studied metal complexes of the new derivative with zinc(II), copper(II) and iron(II). We also determined the antiproliferative activities of the HAtpy derivative and its metal complexes in human cell lines A2780 (ovary, adenocarcinoma, HTL98008), A549 (lung, carcinoma, HTL03001), MDA-MB-453 (breast, carcinoma, HTL01013), SKHep1 (liver, carcinoma) and compared them to free tpy systems. The polysaccharide backbone confers water solubility to the tpy-based system and may extend the application of tpy chemistry in water solutions.

2. Materials and methods

2.1. Materials

Commercially available reagents were used directly unless otherwise noted. Hyaluronic acid (~30 units, 8–15 kDa) was purchased from Carbosynth, 4′-Chloro-2,2′:6′,2″-terpyridine (TpyCl) and DMTMM (4-(4,6-dimethoxy-1,3,5-triazin-2-yl)-4-methylmorpholinium chloride) were purchased from TCI (Tokyo, Japan).

3-([2,2′:6′,2″-terpyridin]-4′-yloxy)propan-1-amine ($TpyNH_2$) was synthesised as reported elsewhere [48].

TLC (Thin layer chromatography) was carried out on silica gel plates (Merck 60-F254). Carbohydrate derivatives were detected on TLC with UV light and the anisaldehyde test.

2.2. NMR spectroscopy

^{1}H NMR spectra were recorded with a Varian UNITY PLUS-500 spectrometer at 499.9 MHz at 300 K, using standard pulse programs from the Varian library.

2.3. UV–Vis spectroscopy

UV–Vis spectra were recorded with a Cary 3500 UV-Vis spectrophotometer equipped with a Peltier temperature control module.

UV–Vis titrations were carried out in phosphate buffer (pH = 7.4). HAtpy was dissolved in the buffer. Freshly prepared $FeSO_4$ solution in 2 mM H_2SO_4, $Zn(ClO_4)_2$ and $Cu(NO_3)_2$ were used. The titrant (metal solution) was added by a Hamilton micro-syringe to the solution of the ligand in the cuvette, under stirring at 25 °C.

2.4. Dynamic light scattering

Dynamic light scattering (DLS) measurements were performed with Zetasizer Nano ZS (Malvern Instruments, UK) operating at 633 nm (He–Ne laser) at 25 °C. The mean hydrodynamic diameter (d) of the NPs was calculated from intensity measurement after averaging ten measurements. The samples (4 mg/ml) were prepared in phosphate buffer (pH 7.4) in ultrapure filtered water (0.2 μm filter).

2.5. Synthesis of HAtpy

HA (150 mg, 0.013 mmol) was dissolved in 15 ml of MilliQ water. An aqueous solution of DMTMM (128 mg, 0.463 mmol) and an acetonitrile solution of $TpyNH_2$ (142 mg, 0.40 mmol) were prepared. DMTMM and $TpyNH_2$ were added to the HA solution under stirring.

After about 12 h, unreacted $TpyNH_2$ precipitated. The white solid was eliminated by centrifugation. The supernatant solution was purified through a Sephadex G-15 column eluted with MilliQ water.

^{1}H NMR (500 MHz, D_2O) δ(ppm): 8.86–8.66 (br. s, H6, H6″, H3, H3″ of tpy), 8.62–6.35 (br. s, H3′, H5′, H4, H4″ of tpy), 7.97–7.76 (br. s, H5, H5″ of tpy), 4.46 (br. s, H-1 of D-glucuronic acid unit), 4.39 (s, H-1 of *N*-acetyl-D-glucosamine unit), 4.34 (sh, a of propylenic linker), 3.89–3.12 (m, H-2, H-3, H-4, H-5, H-6 of HA backbone and c of propylenic linker), 2.06 (m, b of propylenic linker), 1.91 (s, CH_3 of HA).

2.6. Synthesis of HAtpy metal complexes

Cu^{2+}, Fe^{2+} and Zn^{2+} complexes were synthesised by adding respectively $Cu(NO_3)_2$, $FeSO_4$ or $Zn(ClO_4)_2$ water solution to the ligand water solution in a 1:2 M/L (L is tpy unit) molar ratio. Ternary complexes were synthesised by adding $Cu(NO_3)_2$, $FeSO_4$ or $Zn(ClO_4)_2$ water solution to HAtpy and TpyCl in water/DMSO 10/1 solution at a M/L/TpyCl 1:1:1 (L is tpy unit) molar ratio.

HAtpy-Cu-TpyCl: UV–Vis spectrum λ nm (ε, L $M^{-1}cm^{-1}$): 270 (sh, 96000), 276 (97300), 286 (85300), 312 (sh, 45300), 325 (60000), 337 (54700).

HAtpy-Fe-TpyCl: UV–Vis spectrum λ nm (ε, L $M^{-1}cm^{-1}$): 273 (111000), 282 (sh, 93300), 316 (97300), 509 (sh, 16000), 558 (25300).

HAtpy-Zn-TpyCl: UV–Vis spectrum λ nm (ε, L $M^{-1}cm^{-1}$): 266 (sh, 86700), 274 (94700), 282 (89300), 322 (82700), 330 (68000).

2.7. Evaluation of the antiproliferative activity

Human cell lines A2780 (ovary, adenocarcinoma, HTL98008), A549 (lung, carcinoma, HTL03001), MDA-MB-453 (breast, carcinoma, HTL01013) (all these cell lines obtained from Interlab Cell Line Collection, Genova, Italy), and SKHep1 (liver, carcinoma, 52 HTB, obtained from American Type Culture Collection, Rockville, MA, USA), were plated in 180 μl into flat-bottomed 96-well microtiter plates at the opportune numbers per well in complete media (RPMI 1640 or DMEM) added with antibiotics and 10 % fetal bovine serum (FBS). After 6–8 h, cells were administered with 20 μl containing five concentrations of HAtpy derivatives diluted in water plus 0.75 % DMSO.

Plates were then processed as described elsewhere [49]. The NP

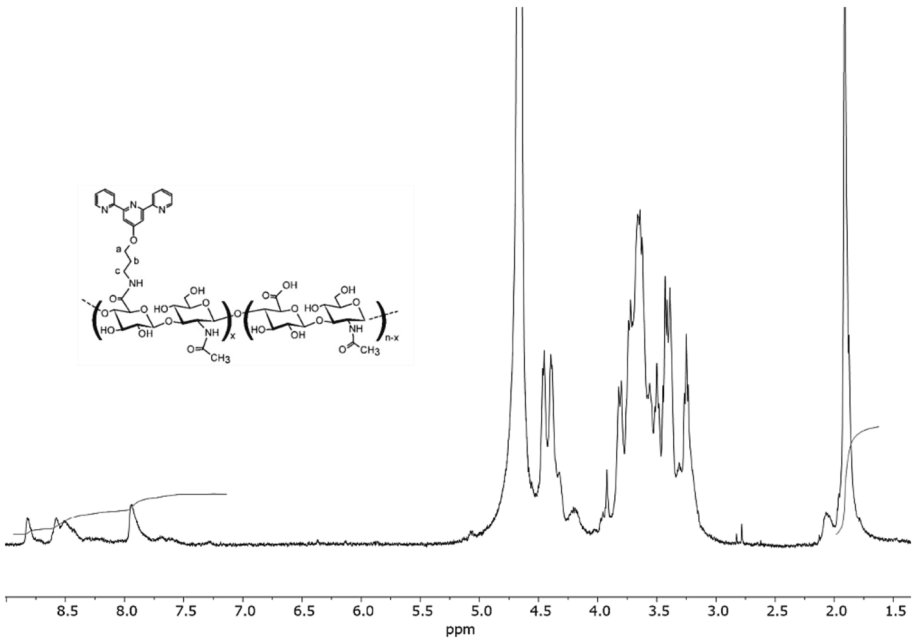

Fig. 2. ^{1}H NMR spectrum of HAtpy (D_2O, 500 MHz).

concentrations inhibiting 50 % cell growth (IC_{50}) were calculated based on the analysis of the concentration–response curves. Each experiment was repeated 4–5 times. IC_{50} values higher than 30 μM were considered pharmacologically irrelevant.

2.8. Statistical analysis of data

The Student's *t*-test for parametric data was used for statistical comparisons.

3. Results and discussion

HAtpy conjugate was synthesised by coupling HA with $TpyNH_2$ by amidation reaction, using DMTMM as the coupling agent (Fig. S1).

^{1}H NMR and UV–vis spectroscopy confirmed the conjugation of tpy with HA. The ^{1}H NMR spectrum of HAtpy (Fig. 2 and S2) shows broad signals, as typically found for polymers. ^{1}H NMR spectrum of HA is reported for comparison in Fig. S2.

In the ^{1}H NMR spectrum, the broad peaks between 8.86 and 7.76 ppm are due to the tpy protons. H-1 protons of the D-glucuronic acid and *N*-acetyl-D-glucosamine of HA resonate at 4.5–4.3 ppm. Other HA protons resonate from 4.0 to 3.0 ppm. The signal at 1.91 ppm was assigned to the methyl group in the HA backbone. The b CH_2 of the propylenic chain of the tpy linker resonates at 2.06 ppm. Other CH_2 resonances (a and c) overlap with HA signals (3.5 and 4.3 ppm). From the integration of aromatic signals of tpy and $–CH_3$ of HA, a degree of functionalisation of about 25 % was estimated (about 7 of the 30 repeating disaccharide units of HA were functionalised with tpy).

UV–vis spectrum of the HAtpy ligand showed bands at 240 and 280 nm with a shoulder at 300 nm due to π-π* transitions, as reported for tpy (Fig. S3).

The particle size distribution of HAtpy was investigated with DLS. HAtpy forms NPs in water at pH 7.4. The DLS spectra of HAtpy showed a main population with a diameter of the hydrodynamic volume 8 nm ± 4 nm (Fig. S4, Z-average 11 nm). The functionalisation of HA with tpy did not change the size of the nanoparticles but its peak size distribution (HA diameter is 9 nm ± 4 nm, Z-average 26 nm).

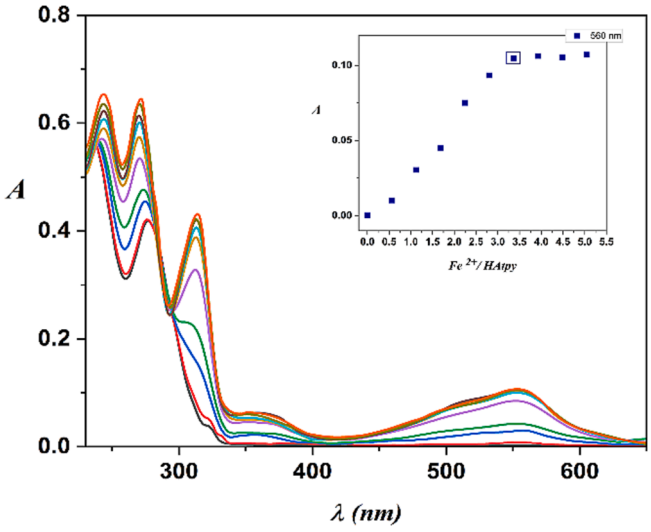

Fig. 3. UV–Vis spectrophotometric titration of HAtpy ($6.0x10^{-6}$ M, phosphate buffer pH 7.4) with Fe^{2+}. Inset: Absorbance at 560 nm upon the addition of Fe^{2+}.

3.1. Metal complexes of HAtpy

To study the complexation properties of HAtpy, we carried out UV–Vis titrations of HAtpy with M^{2+} salt solutions (M = Fe, Cu, Zn) in phosphate buffer at pH = 7.4. The titration curves showed characteristic bands.

During the titration, a new band arose at about 313 nm (Fig. 3). This band is characteristic of the conformational change of tpy from the trans/trans conformation of the free ligand to the perfectly planarised cis/cis conformation in the complex [50].

In the case of the Fe^{2+} system, an intense band appeared in the visible region at 560 nm due to a metal-to-ligand charge transfer (MLCT). The titration showed a clear isosbestic point at about 300 nm, suggesting that only two species, the free ligand and the metal complex, are present during the titration process. Spectra changed up to a Fe^{2+}/HAtpy 3.5 or Fe^{2+}/L (L is tpy unit) 1:2 ratio (Fig. 3), considering the

Table 1
IC_{50} values (μM) of HAtpy, its binary Cu^{2+}, Fe^{2+} and Zn^{2+} complexes (M/L 1:2) and ternary complexes with TpyCl (M/L/TpyCl 1:1:1, L is tpy unit)). $[M(TpyCl)_2]^{2+}$ are reported for comparison.

Cell lines	HAtpy	HAtpy-Fe	HAtpy-Cu	HAtpy-Zn	HAtpy-Fe-TpyCl	HAtpy-Cu-TpyCl	HAtpy-Zn-TpyCl	TpyCl	$[Fe(TpyCl)_2]^{2+}$	$[Cu(TpyCl)_2]^{2+}$	$[Zn(TpyCl)_2]^{2+}$
A2780	4.91 ± 0.97	>30	6.68 ± 2.88	>30	0.17 ± 0.02[a]	0.04 ± 0.02[b]	0.12 ± 0.04[c]	0.31 ± 0.08	0.22 ± 0.04	0.26 ± 0.01	0.06 ± 0.01[e]
A549	4.45 ± 0.94	>30	>30	>30	0.51 ± 0.09[b]	0.05 ± 0.01[b]	0.06 ± 0.01	0.42 ± 0.19	0.26 ± 0.05	0.28 ± 0.02	0.04 ± 0.01[e]
SKHep1	11.5 ± 1.0	1.74 ± 0.66	>30	ND	>30	>30	ND	0.64 ± 0.26	0.45 ± 0.14	0.32 ± 0.14	ND
MDA-MB-453	2.68 ± 0.85	>30	29.4 ± 8.4	>30	13.9 ± 3.9	0.09 ± 0.01[b]	0.12 ± 0.02[d]	1.40 ± 0.58	1.47 ± 0.70	1.33 ± 0.33	0.06 ± 0.01[e]

[a] $p < 0.05$ as compared to the treatment with $[Fe(TpyCl)_2]^{2+}$; [b]$p < 0.01$, as compared to the treatment with $[Cu(TpyCl)_2]^{2+}$; [c]$p < 0.02$, as compared to the treatment with $[Zn(TpyCl)_2]^{2+}$; [d]$p < 0.001$, as compared to the treatment with $[Zn(TpyCl)_2]^{2+}$; [e]$p < 0.001$, as compared to the treatment with $[Fe(TpyCl)_2]^{2+}$ and $[Cu(TpyCl)_2]^{2+}$.

functionalisation degree of HA obtained by NMR spectra. It suggests that $[Fe(L)_2]^{2+}$ complex is the main species. Hence, as reported for free terpyridine ligand, two tpy moieties are coordinated to Fe^{2+} in an ML_2-like coordination environment [50]. Metal coordination can occur between tpy units intramolecularly within the same HAtpy molecule or intermolecularly in different HAtpy molecules.

As for Zn^{2+}complexes, in the UV–Vis spectra, a well-developed bimodal band increases in the region between 310 and 322 nm and the isosbestic point is evident at 300 nm (Fig. S6). The spectra are characterised by a straight slope of the absorbance values at 322 nm versus metal ion concentration and an abrupt saturation at a 1/2 M/L (L is tpy unit) ratio.

A similar trend was found when Cu^{2+} was added to the HAtpy solution (Fig. S7). Isosbestic point is present up to 0.5 equivalents of Cu^{2+}. When Cu^{2+}/tpy unit ratio > 0.5, spectra are subjected to bathochromic shift (Fig. S7) and the intensity of the bands between 310 and 320 nm decreased. The titration of HAtpy with copper (II) is the only example where a significant spectral change can be observed in the range of M/L ratio between 0.5 and 1 due to the coexistence of ML and ML_2 species (Fig. S8). CuL and CuL_2 species have been characterised in the case of terpyridine ligands [11,51].

UV–Vis spectra of ternary complexes HAtpy-M-TpyCl are reported in Fig. S9. The spectra are similar to the ML_2 spectra.

The particle size distribution of HAtpy-M^{2+} (M = Fe, Cu, Zn) was investigated by DLS. The addition of metal ions revealed an increase in the hydrodynamic volume compared to the ligand (Fig. S5, Table S1). This is in keeping with the formation of intermolecular complex species. HAtpy-Cu^{2+} showed the smallest Z-average (18 nm, Table S1), which may be due to the small amount of ML species. HAtpy-Fe^{2+} and HAtpy-Zn^{2+} NPs showed a higher hydrodynamic volume (Z-average is 25 nm and 30 nm respectively), which may suggest the formation of intermolecular ML_2 species (Table S1, Fig. S5). Similar behaviour has been reported for other tpy polymers [52].

3.2. Antiproliferative activity

The antiproliferative activity of HAtpy and its Fe^{2+}, Cu^{2+} and Zn^{2+} binary and ternary complexes with TpyCl (Fig. S10) was studied in MDA-MB-453, SKHep1 (except for Zn complexes), A549, and A2780 cell lines (Table 1). We have already investigated Fe^{2+} and Cu^{2+} TpyCl complexes [18]. The antiproliferative activity of $[Zn(TpyCl)_2]^{2+}$ [53] was studied for comparison. The results are reported in Table 1.

Data showed that HAtpy has IC_{50} values that are pharmacologically significant in all cell lines tested, although higher than TpyCl. Binary complexes of HAtpy were generally pharmacologically inactive on all cell lines except HAtpy-Fe^{2+}, which showed significant IC_{50} of about 1.74 ± 0.66 μM in SKHep1 cells. A similar trend was found for cross-linked cyclodextrin polymers functionalised with tpy [48].

On the contrary, ternary complexes had a high antiproliferative activity on all cell lines except for SKHep1 cells (IC_{50}s > 30 μM) and HAtpy-Fe-TpyCl in MDA-MB-453 cells (IC_{50}, 13.9 ± 3.9 μM).

It is noteworthy that the treatment with the ternary complex HAtpy-Cu-TpyCl caused a significant reduction of IC_{50} values in MDA-MB-453, A549 and A2780 cells, compared to the treatment with $[Cu(TpyCl)_2]^{2+}$. In MDA-MB-453, the IC_{50} value of HAtpy-Cu-TpyCl (0.09 ± 0.01 μM) is lower than that we found for Doxorubicin (0.18 μM) [48].

The ternary complex HAtpy-Fe-TpyCl showed an IC_{50} value slightly lower than $[Fe(TpyCl)_2]^{2+}$ only in the A2780 cell line. Regarding $[Zn(TpyCl)_2]^{2+}$, its activity was consistently higher than that of the analogous Cu^{2+} and Fe^{2+} complexes (Table 1). $[Zn(TpyCl)_2]^{2+}$ showed IC_{50} values lower (A2780 and MDA-MB-453 cells) or similar (A549 cells) than the corresponding ternary complex HAtpy-Zn-TpyCl.

4. Conclusions

The new hyaluronic acid functionalised with terpyridine units can form metal complexes with Fe^{2+}, Zn^{2+} and Cu^{2+}. We studied the antiproliferative activity of the conjugate and its binary and ternary complexes with 4-chloro-terpyridine in cancer cells. The HAtpy-M-TpyCl complexes showed antiproliferative activity in the nM range, in dependence of the cell line. In particular, HAtpy-Cu-TpyCl IC_{50}s were lower than $[Cu(TpyCl)_2]^{2+}$. Specifically, the ternary copper complex showed the best improvement of the antiproliferative activity in MDA-MB-453 cells, and the IC_{50} value was lower than that of Doxorubicin.

Drawing from the antiproliferative activity data of ternary complexes in comparison to $[Fe(TpyCl)_2]^{2+}$ and $[Cu(TpyCl)_2]^{2+}$, we may propose that the presence of hyaluronic acid may enhance the cellular uptake of the copper complex (in three of the four cell lines), and of the iron complex (in one of the four cell lines). In the case of HAtpy-Zn-TpyCl, the hyaluronic acid moiety did not improve the cytotoxicity compared to $[Zn(TpyCl)_2]^{2+}$.

The conjugation with hyaluronic acid is a fruitful approach for improving the water-solubility of terpyridine and their metal complexes. The coordination properties of terpyridine ligand can be extended to other tpy derivatives by tuning the properties of the final system.

5. Authorship contributions

R. Panebianco: Data curation, Investigation, Original draft, Writing – review & editing. **M. Viale:** Data curation, Formal analysis, Investigation, Writing – review & editing. **Graziella Vecchio:** Supervision, Data curation, Investigation, Original Draft Writing – review & editing.

Declaration of competing interest

The authors declare that they have no known competing financial interests or personal relationships that could have appeared to influence the work reported in this paper.

Data availability

Data will be made available on request.

Acknowledgements

The authors acknowledge support from the Italian Ministero dell'Università e della Ricerca (MUR) Italy, (PON03PE_00216_1), EU funding within the NextGeneration EU-MUR PNRR Extended Partnership initiative on Emerging Infectious Diseases (Project no. PE00000007, INF-ACT) and the Italian Ministry of Health, Italy, under grant "Ricerca Corrente", 2022-2772566.

Appendix A. Supplementary data

Supplementary data to this article can be found online at https://doi.org/10.1016/j.poly.2023.116793.

References

[1] R. Paprocka, M. Wiese-Szadkowska, S. Janciauskiene, T. Kosmalski, M. Kulik, A. Helmin-Basa, Latest developments in metal complexes as anticancer agents, Coord. Chem. Rev. 452 (2022), 214307, https://doi.org/10.1016/j.ccr.2021.214307.

[2] E.U. Mughal, M. Mirzaei, A. Sadiq, S. Fatima, A. Naseem, N. Naeem, N. Fatima, S. Kausar, A.A. Altaf, M.N. Zafar, B.A. Khan, Terpyridine-metal complexes: effects of different substituents on their physico-chemical properties and density functional theory studies, R. Soc. Open Sci. 7 (2020), 201208, https://doi.org/10.1098/rsos.201208.

[3] Y. Tang, M. Kong, X. Tian, J. Wang, Q. Xie, A. Wang, Q. Zhang, H. Zhou, J. Wu, Y. Tian, A series of terpyridine-based zinc(II) complexes assembled for third-order nonlinear optical responses in the near-infrared region and recognizing lipid membranes, J. Mater. Chem. B 5 (2017) 6348–6355, https://doi.org/10.1039/C7TB01063J.

[4] A. Winter, M. Gottschaldt, G.R. Newkome, U.S. Schubert, Terpyridines and their Complexes with First Row Transition Metal Ions:Cytotoxicity, Nuclease Activity and Self-Assembly of Biomacromolecules, Curr. Top. Med. Chem. 12 (2012) 158–175, https://doi.org/10.2174/156802612799078919.

[5] J. Karges, O. Blacque, M. Jakubaszek, B. Goud, P. Goldner, G. Gasser, Systematic investigation of the antiproliferative activity of a series of ruthenium terpyridine complexes, J. Inorg. Biochem. 198 (2019), 110752, https://doi.org/10.1016/j.jinorgbio.2019.110752.

[6] X. Liang, J. Jiang, X. Xue, L. Huang, X. Ding, D. Nong, H. Chen, L. Pan, Z. Ma, Synthesis, characterization, photoluminescence, anti-tumor activity, DFT calculations and molecular docking with proteins of zinc(ii) halogen substituted terpyridine compounds, Dalton Trans. 48 (2019) 10488–10504, https://doi.org/10.1039/C8DT04924F.

[7] L. Huang, R. Liu, J. Li, X. Liang, Q. Lan, X. Shi, L. Pan, H. Chen, Z. Ma, Synthesis, characterization, anti-tumor activity, photo-luminescence and BHb/HHb/Hsp90 molecular docking of zinc(II) hydroxyl-terpyridine complexes, J. Inorg. Biochem. 201 (2019), 110790, https://doi.org/10.1016/j.jinorgbio.2019.110790.

[8] S. Roy, S. Roy, S. Saha, R. Majumdar, R.R. Dighe, E.D. Jemmis, A.R. Chakravarty, Cobalt(ii) complexes of terpyridine bases as photochemotherapeutic agents showing cellular uptake and photocytotoxicity in visible light, Dalton Trans. 40 (2011) 1233–1242, https://doi.org/10.1039/C0DT00223B.

[9] L. Gourdon, K. Cariou, G. Gasser, Phototherapeutic anticancer strategies with first-row transition metal complexes: a critical review, Chem. Soc. Rev. 51 (2022) 1167–1195, https://doi.org/10.1039/D1CS00609F.

[10] X. Guan, H. Wen, B. Wang, Z. Wang, Y. Zhou, H. Liu, H. Chen, L. Pan, Z. Ma, Anticancer activities and DNA/BSA interactions for five Cu(II) compounds with substituted terpyridine ligands, J. Coord. Chem. 76 (2023) 667–688, https://doi.org/10.1080/00958972.2023.2209270.

[11] J. Karges, K. Xiong, O. Blacque, H. Chao, G. Gasser, Highly cytotoxic copper(II) terpyridine complexes as anticancer drug candidates, Inorg. Chim. Acta 516 (2021), 120137, https://doi.org/10.1016/J.ICA.2020.120137.

[12] Z. Ma, L. Wei, E.C.B.A. Alegria, L.M.D.R.S. Martins, M.F.C. Guedes da Silva, A.J. L. Pombeiro, Synthesis and characterization of copper(<scp>ii</scp>) 4′-phenyl-terpyridine compounds and catalytic application for aerobic oxidation of benzylic alcohols, Dalton Trans. 43 (2014) 4048–4058, https://doi.org/10.1039/C3DT53054J.

[13] C.E. Housecroft, E.C. Constable, The terpyridine isomer game: from chelate to coordination network building block, Chem. Commun. 56 (2020) 10786–10794, https://doi.org/10.1039/D0CC04477F.

[14] R. Dobrawa, P. Ballester, C. Saha-Moller, F. Wurthner, Thermodynamics of 2,2 ': 6 ',2 ' '-terpyridine-meta1 ion complexation, ACS Symp. Ser. (2006) 43–62, https://doi.org/10.1021/bk-2006-0928.ch004.

[15] Y. Yang, F.-F. Guo, C.-F. Chen, Y.-L. Li, H. Liang, Z.-F. Chen, Antitumor activity of synthetic three copper(II) complexes with terpyridine ligands, J. Inorg. Biochem. 240 (2023), 112093, https://doi.org/10.1016/j.jinorgbio.2022.112093.

[16] E.A. Hassan, W.S. Abou Elseoud, M.T. Abo-Elfadl, M.L. Hassan, New pectin derivatives with antimicrobial and emulsification properties via complexation with metal-terpyridines, Carbohydr. Polym. 268 (2021), 118230, https://doi.org/10.1016/j.carbpol.2021.118230.

[17] M.M. Elnagar, S. Samir, Y.M. Shaker, A.A. Abdel-Shafi, W. Sharmoukh, M.S. Abdel-Aziz, K.S. Abou-El-Sherbini, Synthesis, characterization, and evaluation of biological activities of new 4′-substituted ruthenium (II) terpyridine complexes: Prospective anti-inflammatory properties, Appl. Organomet. Chem. 35 (2021) e6024.

[18] R. Panebianco, M. Viale, F. Loiacono, V. Lanza, D. Milardi, G. Vecchio, Terpyridine Glycoconjugates and Their Metal Complexes: Antiproliferative Activity and Proteasome Inhibition, ChemMedChem 18 (2023) e202200701.

[19] K. Choroba, B. Machura, A. Szlapa-Kula, J.G. Malecki, L. Raposo, C. Roma-Rodrigues, S. Cordeiro, P.V. Baptista, A.R. Fernandes, Square planar Au(III), Pt(II) and Cu(II) complexes with quinoline-substituted 2,2′:6′,2″-terpyridine ligands: From in vitro to in vivo biological properties, Eur. J. Med. Chem. 218 (2021), 113404, https://doi.org/10.1016/j.ejmech.2021.113404.

[20] K. Malarz, D. Zych, M. Kuczak, R. Musioł, A. Mrozek-Wilczkiewicz, Anticancer activity of 4′-phenyl-2,2′:6′,2″-terpyridines – behind the metal complexation, Eur. J. Med. Chem. 189 (2020), 112039, https://doi.org/10.1016/j.ejmech.2020.112039.

[21] J. Jiang, J. Li, C. Liu, R. Liu, X. Liang, Y. Zhou, L. Pan, H. Chen, Z. Ma, Study on the substitution effects of zinc benzoate terpyridine complexes on photoluminescence, antiproliferative potential and DNA binding properties, J. Biol. Inorg. Chem. 25 (2020) 311–324, https://doi.org/10.1007/s00775-020-01763-6.

[22] J. Li, H. Yan, Z. Wang, R. Liu, B. Luo, D. Yang, H. Chen, L. Pan, Z. Ma, Copper chloride complexes with substituted 4′-phenyl-terpyridine ligands: synthesis, characterization, antiproliferative activities and DNA interactions, Dalton Trans. 50 (2021) 8243–8257, https://doi.org/10.1039/D0DT03989F.

[23] J. Grau, A. Caubet, O. Roubeau, D. Montpeyó, J. Lorenzo, P. Gamez, Time-Dependent Cytotoxic Properties of Terpyridine-Based Copper Complexes, Chembiochem 21 (2020) 2348–2355, https://doi.org/10.1002/cbic.202000154.

[24] Z. Feng, D. Zhang, H. Guo, W. Su, Y. Tian, X. Tian, Lighting up RNA-specific multi-photon and super-resolution imaging using a novel zinc complex, Nanoscale 15 (2023) 5486–5493, https://doi.org/10.1039/D2NR05392F.

[25] K. Velugula, A. Kumar, J.P. Chinta, Nuclease and anticancer activity of antioxidant conjugated terpyridine metal complexes, Inorg. Chim. Acta 507 (2020), 119596, https://doi.org/10.1016/j.ica.2020.119596.

[26] C. Li, F. Xu, Y. Zhao, W. Zheng, W. Zeng, Q. Luo, Z. Wang, K. Wu, J. Du, F. Wang, Platinum(II) Terpyridine Anticancer Complexes Possessing Multiple Mode of DNA Interaction and EGFR Inhibiting Activity, accessed May 29, 2023, Front. Chem. 8 (2020), https://www.frontiersin.org/articles/10.3389/fchem.2020.00210.

[27] Y. Shen, T. Shao, B. Fang, W. Du, M. Zhang, J. Liu, T. Liu, X. Tian, Q. Zhang, A. Wang, J. Yang, J. Wu, Y. Tian, Visualization of mitochondrial DNA in living cells with super-resolution microscopy using thiophene-based terpyridine Zn(ii) complexes, Chem. Commun. 54 (2018) 11288–11291, https://doi.org/10.1039/C8CC06276E.

[28] K.U. Khan, M.U. Minhas, S.F. Badshah, M. Suhail, A. Ahmad, S. Ijaz, Overview of nanoparticulate strategies for solubility enhancement of poorly soluble drugs, Life Sci. 291 (2022), 120301, https://doi.org/10.1016/j.lfs.2022.120301.

[29] Z. Fülöp, T.T. Nielsen, K.L. Larsen, T. Loftsson, Dextran-based cyclodextrin polymers: Their solubilizing effect and self-association, Carbohydr. Polym. 97 (2013) 635–642, https://doi.org/10.1016/j.carbpol.2013.05.053.

[30] A.M. Gomez, J.C. Lopez, Carbohydrates and BODIPYs: access to bioconjugatable and water-soluble BODIPYs, Pure Appl. Chem. 91 (2019) 1073–1083, https://doi.org/10.1515/pac-2019-0204.

[31] T. Mohan, K.S. Kleinschek, R. Kargl, Polysaccharide peptide conjugates: Chemistry, properties and applications, Carbohydr. Polym. 280 (2022), 118875, https://doi.org/10.1016/j.carbpol.2021.118875.

[32] C. Buckley, E.J. Murphy, T.R. Montgomery, I. Major, Hyaluronic Acid: A Review of the Drug Delivery Capabilities of This Naturally Occurring Polysaccharide, Polymers 2022, Vol. 14, Page 3442. 14 (2022) 3442. https://doi.org/10.3390/POLYM14173442.

[33] N.G. Kotla, S.R. Bonam, S. Rasala, J. Wankar, R.A. Bohara, J. Bayry, Y. Rochev, A. Pandit, Recent advances and prospects of hyaluronan as a multifunctional therapeutic system, J. Control. Release 336 (2021) 598–620, https://doi.org/10.1016/j.jconrel.2021.07.002.

[34] M. Dovedytis, Z.J. Liu, S. Bartlett, Hyaluronic acid and its biomedical applications: A review, Eng. Regen. 1 (2020) 102–113, https://doi.org/10.1016/j.engreg.2020.10.001.

[35] L.T. Senbanjo, M.A. Chellaiah, CD44: A multifunctional cell surface adhesion receptor is a regulator of progression and metastasis of cancer cells, Front. Cell Dev. Biol. 5 (2017) 18, https://doi.org/10.3389/fcell.2017.00018.

[36] M.K. Cowman, H.G. Lee, K.L. Schwertfeger, J.B. McCarthy, E.A. Turley, The content and size of hyaluronan in biological fluids and tissues, Front. Immunol. 6 (2015), https://doi.org/10.3389/fimmu.2015.00261.

[37] X. Yang, I. Dogan, V.R. Pannala, S. Kootala, J. Hilborn, D. Ossipov, A hyaluronic acid-camptothecin nanoprodrug with cytosolic mode of activation for targeting cancer, Polym. Chem. 4 (2013) 4621–4630, https://doi.org/10.1039/c3py00402c.

[38] M. Ashrafizadeh, S. Mirzaei, M.H. Gholami, F. Hashemi, A. Zabolian, M. Raei, K. Hushmandi, A. Zarrabi, N.H. Voelcker, A.R. Aref, M.R. Hamblin, R.S. Varma, S. Samarghandian, I.J. Arostegi, M. Alzola, A.P. Kumar, V.K. Thakur, N. Nabavi, P. Makvandi, F.R. Tay, G. Orive, Hyaluronic acid-based nanoplatforms for Doxorubicin: A review of stimuli-responsive carriers, co-delivery and resistance suppression, Carbohydr. Polym. 272 (2021) 144–8617, https://doi.org/10.1016/J.CARBPOL.2021.118491.

[39] V. Machado, M. Morais, R. Medeiros, Hyaluronic Acid-Based Nanomaterials Applied to Cancer: Where Are We Now? Pharmaceutics 14 (2022) 2092, https://doi.org/10.3390/pharmaceutics14102092.
[40] G. Huang, H. Huang, Application of hyaluronic acid as carriers in drug delivery, Drug Deliv. 25 (2018) 766–772, https://doi.org/10.1080/10717544.2018.1450910.
[41] N.G. Kotla, I.L. Mohd Isa, A. Larrañaga, B. Maddiboyina, S.K. Swamy, G. Sivaraman, P.K. Vemula, Hyaluronic Acid-Based Bioconjugate Systems, Scaffolds, and Their Therapeutic Potential, Advanced Healthcare Materials. n/a (n.d.) 2203104. https://doi.org/10.1002/adhm.202203104.
[42] R. Barbucci, A. Magnani, S. Lamponi, S. Mitola, M. Ziche, L. Morbidelli, F. Bussolino, Cu(II) and Zn(II) complexes with hyaluronic acid and its sulphated derivative. Effect on the motility of vascular endothelial cells, J. Inorg. Biochem. 81 (2000) 229–237, https://doi.org/10.1016/s0162-0134(00)00127-6.
[43] A.L.R. Mercê, L.C. Marques Carrera, L.K. Santos Romanholi, M.Á. Lobo Recio, Aqueous and solid complexes of iron(III) with hyaluronic acid: Potentiometric titrations and infrared spectroscopy studies, J. Inorg. Biochem. 89 (2002) 212–218, https://doi.org/10.1016/S0162-0134(01)00422-6.
[44] K. Burger, J. Illés, B. Gyurcsik, M. Gazdag, E. Forrai, I. Dékány, K. Mihályfi, Metal ion coordination of macromolecular bioligands: formation of zinc(II) complex of hyaluronic acid, Carbohydr. Res. 332 (2001) 197–207, https://doi.org/10.1016/S0008-6215(01)00065-9.
[45] B. Tao, Z. Yin, Redox-Responsive Coordination Polymers of Dopamine-Modified Hyaluronic Acid with Copper and 6-Mercaptopurine for Targeted Drug Delivery and Improvement of Anticancer Activity against Cancer Cells, Polymers 12 (2020) 1132, https://doi.org/10.3390/polym12051132.
[46] R. Buffa, J. Běťák, S. Kettou, M. Hermannová, L. Pospíšilová, V. Velebný, A novel DTPA cross-linking of hyaluronic acid and metal complexation thereof, Carbohydr. Res. 346 (2011) 1909–1915, https://doi.org/10.1016/j.carres.2011.04.015.
[47] V. Greco, I. Naletova, I.M.M. Ahmed, S. Vaccaro, L. Messina, D. La Mendola, F. Bellia, S. Sciuto, C. Satriano, E. Rizzarelli, Hyaluronan-carnosine conjugates inhibit Aβ aggregation and toxicity, Sci. Rep. 10 (2020) 15998, https://doi.org/10.1038/s41598-020-72989-2.
[48] R. Panebianco, M. Viale, N. Bertola, F. Bellia, G. Vecchio, Terpyridine functionalized cyclodextrin nanoparticles: metal coordination for tuning anticancer activity, Dalton Trans. 51 (2022) 5000–5003, https://doi.org/10.1039/D2DT00613H.
[49] C. Dell'Erba, B. Chiavarina, C. Fenoglio, G. Petrillo, C. Cordazzo, E. Boncompagni, D. Spinelli, E. Ognio, C. Aiello, M.A. Mariggiò, M. Viale, Inhibition of cell proliferation, cytotoxicity and induction of apoptosis of 1,4-bis(1-naphthyl)-2,3-dinitro-1,3-butadiene in gastrointestinal tumour cell lines and preliminary evaluation of its toxicity in vivo, Pharmacol. Res. 52 (2005) 271–282, https://doi.org/10.1016/j.phrs.2005.03.011.
[50] R. Dobrawa, P. Ballester, C.R. Saha-Möller, F. Würthner, Thermodynamics of 2,2′:6′,2″-Terpyridine-Metal Ion Complexation, in: 2006: pp. 43–62. https://doi.org/10.1021/bk-2006-0928.ch004.
[51] A. Meyer, G. Schnakenburg, R. Glaum, O. Schiemann, (Bis(terpyridine))copper(II) Tetraphenylborate: A Complex Example for the Jahn-Teller Effect, Inorg. Chem. 54 (2015) 8456–8464, https://doi.org/10.1021/acs.inorgchem.5b01157.
[52] H. Hofmeier, U.S. Schubert, Supramolecular Branching and Crosslinking of Terpyridine-Modified Copolymers: Complexation and Decomplexation Studies in Diluted Solution, Macromol. Chem. Phys. 204 (2003) 1391–1397, https://doi.org/10.1002/macp.200350003.
[53] R.A. Adrian, S.J. Ibarra, H.D. Arman, Bis(4′-chloro-2,2′:6′,2″-terpyridine-κ3N, N′, N″)zinc(II) bis-(tri-fluoro-methane-sulfonate), IUCrData. 7 (2022), x221096, https://doi.org/10.1107/S2414314622010963.